MutS Switches Between Two Fundamentally Distinct Clamps during Mismatch Repair

Cherlhyun Jeong[1,*], **Won–Ki Cho**[1,*], **Kyung–Mi Song**[2], **Christopher Cook**[3], **Tae–Young Yoon**[4], **Changill Ban**[2], **Richard Fishel**[3,5], and **Jong–Bong Lee**[1,6]

[1] Department of Physics, Pohang University of Science and Technology (POSTECH), Pohang, Kyungbuk 790–784, Korea

[2] Department of Chemistry, Pohang University of Science and Technology (POSTECH), Pohang, Kyungbuk 790–784, Korea

[3] Department of Molecular Virology, Immunology and Medical Genetics, The Ohio State University Medical Center, Columbus, OH 43210

[4] Department of Physics and KAIST Institute for the BioCentury, KAIST, Yuseong–gu, Daejeon 305–701, Korea

[5] Physics Department, The Ohio State University, Columbus, OH 43210

[6] School of Interdisciplinary Bioscience and Bioengineering, Pohang University of Science and Technology (POSTECH), Pohang, Kyungbuk 790–784, Korea

Abstract

Single molecule trajectory analysis has suggested DNA repair proteins may perform a 1–dimensional (1D) search on naked DNA encompassing >10,000 nucleotides. Organized cellular DNA (chromatin) presents substantial barriers to such lengthy searches. Using dynamic single molecule fluorescence resonance energy transfer (smFRET) we determined that the mismatch repair (MMR) initiation protein MutS forms a transient clamp that scans duplex DNA for mismatched nucleotides by 1D diffusion for 1 sec (~700 bp) while in continuous rotational contact with the DNA. Mismatch identification provokes ATP binding (3 s) that induces distinctly different MutS sliding clamps with unusual stability on DNA (~600 s), which may be released by adjacent single–stranded DNA (ssDNA). These observations suggest that ATP transforms short–lived MutS lesion scanning clamps into highly stable MMR signaling clamps capable of competing with chromatin and recruiting MMR machinery, yet are recycled by ssDNA excision tracts.

Correspondence: J.–B. Lee (jblee@postech.ac.kr), C. Ban (ciban@postech.ac.kr), or R. Fishel (rfishel@osu.edu).
*Theses authors are equally contributed

Mismatch repair (MMR) recognizes mispairs and lesions in DNA generated by replication errors, chemical or physical damage, and recombination between heteroallelic parental DNAs[1],[2]. The initial recognition of mispairs or lesions is performed by MutS homologs (MSH) and is followed by the recruitment of MutL homologs (MLH/PMS). While there is broad agreement on the engagement of MSH and MLH/PMS in MMR, the mechanics of the downstream events that lead to the specific excision of the mismatch/lesion containing DNA strand are controversial.

DNA excision during MMR is initiated at a single–stranded scission that may be 1000s of nucleotides distant from the mismatch[1],[2]. In the gram–negative enteric bacteria *E.coli* the MutH protein generates the strand scission at a transiently hemimethylated GATC Dam–methylase site[1],[2]. The location and details of the strand scission that precisely directs MMR to newly replicated DNA in archaea, eukaryotes, and most other prokaryotes remain a mystery. The most contentious issues surround the question of how MSH proteins identify a mismatch and then transmit this discovery to the distant strand scission site. There are a number of fundamentally different models[3]. The most likely models posit MSH–MLH/PMS movement along the DNA (cis) from the mismatch to the strand scission, which ultimately signals excision repair. A major contributor to competing interpretations has been the wide range of ionic conditions used to study the biochemical processes of MMR[4],[5].

Locating mismatches and lesions in an ocean of duplex genomic DNA is a significant problem for MMR. It has long been recognized that searching for rare marks on DNA would be dramatically accelerated by a 1D mechanism that involves sliding along duplex strands[6],[7]. For DNA repair proteins this process was illustrated by tracking single molecules on lambda DNA[8],[9]. It was estimated that a 1D search by the yeast MutS homolog (MSH), Msh2–Msh6, could proceed for 10's of thousands of nucleotides[9]. Such an extended search seems improbably since the chromosomes in all organisms are composed of complex protein–DNA structures (chromatin) that would present substantial barriers to 1D diffusion and ultimately the signaling processes required to complete MMR[10]. A rotational diffusion tracking mechanism for the MSH search process has been proposed but remains unconfirmed[9].

Biology requires dynamic molecular organization despite the fundamental thermodynamic tendency toward lower energy and increased entropy. It has been recently recognized that introducing barriers to Brownian motion might favor molecular organization. This could be systematically accomplished by controlled allosteric binding of biologically relevant small molecules that ultimately induce irreversible protein conformational transitions (Rectified Brownian Motion or RTB)[11]. While RTB has been theoretically applied to a number of biological processes including the directional motion of kinesin proteins along intermediate filaments[12], its generality as a driving mechanism in biology has remained enigmatic.

Here we have examined the *Thermus aquaticus (Taq)* MutS search and signaling mechanisms on single DNA molecules as a model for MSH protein functions. We found that MutS transiently ensnares duplex DNA and performs rapid 1 s (~700 bp) searches by 1D rotational diffusion at physiological ionic while in continuous contact with the DNA backbone[6]. When MutS identifies a mismatch it lingers for 3 s, binds ATP, and forms an

unusually stable sliding clamp that remains associated with the DNA for ~10 min. The use of ATP to organize 3D–1D Brownian events into a long–lived 1D signaling process appears to be an unambiguous example of RTB in Biology.

RESULTS

The dynamics of MutS on single DNA molecules

A smFRET[13] assay was developed to investigate the real–time dynamics of MutS on DNA. We used the *Taq* MutS as a model where a single donor fluorophore (Cy3) was conjugated to a cysteine residue within an engineered *Taq* MutS(C42A, T469C) (Fig. 1a, Supplementary Fig. 1). The engineered and Cy3–labeled *Taq* MutS(C42A, T469C) displays identical mismatch binding activity and mismatch–dependent ATP hydrolysis compared to the *wild type Taq* MutS (Supplementary Table 1). A single acceptor fluorophore (Cy5) was attached to a DNA substrate (Fig. 1b; Supplementary Table 2). The immobilization of digoxigenin–antidigoxigenin (Dig–AntiDig) end–blocked Cy5–DNA is described in the Online Methods and illustrated in Fig. 1b. Since the footprint of the *Taq* MutS is 24 bp[14], the protein center may only associate with ~50 bp (17 nm) of a 74 bp DNA substrate. Thus, the distance between the Cy3–Cy5 FRET pairs may range from 4 to 9 nm, and the FRET efficiency may range between 0.9 and 0.1[15],[16]. Single–molecule fluorescent signals were collected using a prism–type total internal reflection fluorescence (TIRF) microscope with a 30 ms time resolution in the presence of an oxygen scavenging system (Online Methods).

The dwell time of MutS on duplex molecules was examined over a wide range of ionic strength. A typical trace of the donor–acceptor pair intensity (Fig. 1c, top panel) and the resulting FRET efficiency (Fig. 1c, bottom panel) is shown. This trace displayed an anti–correlated fluorescent signal of Cy3 (green) and Cy5 (red) that abruptly increased at 5 s, 8 s and 21 s, and fluctuated for 0.6, 0.5, and 2.6 s, respectively, until they disappeared. From numerous similar traces both the dwell time of duplex DNA association ($\tau_{duplex \cdot on}$), the dwell time between successive duplex DNA associations ($\tau_{duplex \cdot off}$), and the FRET efficiency may be collected. The histograms from a population of dwell times fit well with a single–exponential that described the quantitative kinetics between MutS binding ($\tau_{duplex \cdot on}$ = 3.7 ± 0.2 s, mean ± s.e.m.) and successive MutS interactions ($\tau_{duplex \cdot off}$ = 41.4 ± 1.8 s, mean ± s.e.m) on duplex DNA (Fig. 1d).

About 1/3 of the binding events displayed a steady acceptor emission with a very high FRET efficiency (E_{dye} = 0.90 ± 0.12, mean ± s.d.; Supplementary Fig. 2a, b, e) and relatively brief dwell time ($\tau_{dye \cdot on}$ = 6.3 ± 1.6 s, mean ± s.e.m.; at 100 mM KCl). This signal is consistent with a short–lived background interaction between MutS and the alkyl–linked Cy5 fluorophore: an observation consistent with alkylation damage recognition by MSH proteins[17],[18]. The majority of duplex DNA binding events displayed an intermediate FRET efficiency that was easily distinguishable from these high FRET events ($E_{duplex \cdot 74bp \cdot 30ms}$ = 0.48 ± 0.14, mean ± s.d.; Fig. 2a; Supplementary Fig. 2).

MutS searches for mismatches by 1D rotational diffusion

The intermediate FRET events appeared to be the result of time–averaged emission of interfluorophore distances consistent with diffusion of MutS along the entire length of the duplex DNA (Fig. 2a). Such diffusion might be interpreted as a MutS mismatch searching process. To test this hypothesis we independently determined the diffusion coefficient of the Cy3–labeled MutS by examining multiple tracking events along λ phage DNA (Supplementary Fig. 3). These results suggested that MutS may travel the 17 nm effective length of the 74 bp DNA in ~2 ms. To further detail the duplex DNA diffusion events we examined the interaction of MutS with a 100 bp duplex DNA where the 26 nm effective diffusion length might be transited in 4.7 ms (Fig. 2b; Supplementary Table 2). We observed different FRET efficiencies for MutS duplex DNA binding at 30 ms resolution ($E_{\text{duplex·100bp·30ms}} = 0.35 \pm 0.15$, mean ± s.d.; Fig. 2b, left panel) and at 4 ms resolution ($E_{\text{duplex·100bp·4ms}} = 0.33 \pm 0.33$, mean ± s.d.; Fig. 2b, right panel). However, we did not observe any consistent cross–correlation of the fluorophore signals or auto–correlation of FRET values that would further resolve diffusion intermediates.

The change in the FRET efficiency and distribution with DNA length appeared consistent with a searching mechanism in which MutS oscillated on the short duplex DNA substrates used in our studies. To explore this possibility we performed computer simulations based on two hypothetical 1D diffusion models and compared the results to experimental FRET efficiencies determined from 80 individual averaged traces (Fig. 2c; Supplementary Fig. 4). MutS diffusion along the DNA without rotation (Fig. 2c, right panel) appeared unlikely since it predicted very broad FRET distributions with FRET means that were considerably different from the experimental values (Fig. 2c, left panel). However, MutS diffusion with rotation along the DNA (Fig. 2c, middle panel) substantially correlated with the experimental values (Fig. 2c, left panel). Moreover, altering the time resolution was also predictive of the experimental FRET distribution (compare Fig. 2a, b to Supplementary Fig. 4c, e–g). These data support the conclusion that MutS binds duplex DNA and performs a mismatch search by 1D rotational diffusion along the DNA backbone[19].

Searching MutS forms a clamp on the DNA

The off–rate ($k_{\text{duplex·off}} = 1/\tau_{\text{duplex·on}}$) and the on–rate ($k_{\text{duplex·on}} = 1/\tau_{\text{duplex·off}}$) of the duplex DNA at different concentrations of MutS were examined (Fig. 2d). The concentration of MutS (monomer) at which $k_{\text{duplex·off}}$ equals $k_{\text{duplex·on}}$ is the dissociation constant for duplex DNA ($K_{D·\text{duplex}} = 128.2 \pm 12.0$ nM, mean ± s.e.m.). However, the K_D for MutS has been reported to be 2–4 μM in bulk measures and 0.5 μM in AFM studies[20–22]. We reasoned that this inconsistence could be a result of the differences between our double blocked–end DNA substrate and the open–ended DNA substrates used in these previous studies. We found that the dissociation constant dramatically increased with an open–ended DNA ($K_{D·\text{duplex·open}} = 1.30 \pm 0.06$μM, mean ± s.e.m.; Fig. 2e). These results suggest that searching MutS forms a clamp that may be trapped by blocking both duplex DNA ends. Taken as a whole we conclude that MutS topologically ensnares duplex DNA to perform 1D rotational searches along the DNA backbone.

Effect of ionic strength supports continuous association with duplex DNA

A 1D facilitated diffusion search by MutS could occur by two possible mechanisms: 1.) a continuous association with the duplex DNA, or 2.) short intra–strand hops along the duplex DNA. Diffusion by the latter mechanism is predicted to be sensitive to ionic strength since multiple hopping associations must displace ions–of–solvation with each binding event[8]. While we observed a dramatic decrease in dwell time with increasing ionic strength (Supplementary Fig. 5a), the diffusion coefficient appears to remain constant even though ionic strengths above 75 mM made such measures exceedingly difficult (Supplementary Fig. 3). These results appear similar to the 1D facilitated diffusion observations with yeast Msh2–Msh6 and human OGG1 glycosylase, suggesting that MutS is in continuous contact with the DNA during the search along the DNA backbone[8,9]. However, in contrast to these previous studies, the diffusion events appear limited to short ~700 bp stretches at physiological ionic strength ($\tau_{\text{duplex·on}} = 1.0 \pm 0.1$ s at 150 mM KCl, mean $\pm$ s.e.m.; Supplementary Fig. 5a)[9]. In addition, we do not observed an "immobile" state, suggesting that this conformation is either very rare and/or peculiar to long DNAs[9].

Identification of a mismatch by MutS

We introduced a single unpaired thymine (dT) at the 38th nucleotide on the complementary strand and the Cy5 acceptor at the 45th nucleotide from the 5′ –biotin (Fig. 3a; Supplementary Table 2). This arrangement avoided possible interference with surrounding nucleotides that contact MutS residues during mismatch binding (Fig. 3a, see yellow residues). A typical trace of the donor–acceptor pair intensity (Fig. 3b, top panel) and the resulting FRET efficiency (Fig. 3b, bottom panel) for MutS binding to a +dT mismatch DNA is shown. The anti–correlated fluorescent signals of Cy3 (green) and Cy5 (red) abruptly rose at 7 s and 82 s, fluctuated for 5.8 s and 44.8 s, respectively, until they disappeared.

The histogram of FRET efficiency displays a Gaussian distribution with a peak of 0.78 ± 0.16 (mean$\pm$ s.d.; Fig. 3c) that was predicted by computer modeling (Supplementary Fig. 4d). This pattern suggests that the average MutS is located at or near the mismatch. The dwell times from numerous scans fits well with a single–exponential that describes the time between MutS binding ($\tau_{\text{+dT·on}} = 36.5 \pm 3.5$ s, mean $\pm$ s.e.m.) and successive MutS binding ($\tau_{\text{+dT·off}} = 38.1 \pm 1.5$ s, mean $\pm$ s.e.m.) to the +dT mismatched DNA (Fig. 3d). Moreover, mismatch binding was 6–fold longer and completely distinct from background dye binding (Supplementary Fig. 2c–f). We calculated the dissociation constant from the off–rate ($k_{\text{+dT·off}} = 1/\tau_{\text{+dT·on}}$) and the on–rate ($k_{\text{+dT·on}} = 1/\tau_{\text{+dT·off}}$) of the +dT mismatched DNA at different concentrations of MutS ($K_{D,\text{+}dT} = 16.2 \pm 2.1$ nM, mean $\pm$ s.e.m.; Fig. 3e). These results agree well with other single–molecule[20] and bulk[21,22] measures (2 nM–20 nM; Supplementary Table 1).

Observing movement on the duplex DNA surrounding the +dT mismatch was not expected within our time resolution because of the short DNA length and the fast rate of MutS scanning. However, we noted that 16% of the +dT DNA binding events at 30 ms resolution that appeared to contain an intermediate state that occurred prior to the high FRET efficiency associated with MutS mispair binding (Fig. 3f, see dashed lines). This

intermediate state displayed a FRET efficiency of 0.48± 0.12 (mean ± s.d.; Fig. 3g) and is most easily interpreted as MutS diffusing along the duplex DNA prior to mismatch binding. Consistent with this conclusion, we observed more of these searching events at the 4 ms time resolution (30%; Fig. 3j; Supplementary Fig. 6a). For most of these searching events the dwell time was shorter than our resolution time (Fig. 3h and 3i). We also note the lack of a large short–time bin in the $\tau_{+dT\cdot on}$ population (Fig. 3d) and the lack of an appreciable salt dependence on MutS dwell time with a +dT mismatch (Supplementary Fig. 5b) that would be indicative of random binding/dissociation of MutS to a mismatch. Together with our duplex DNA studies, these observations provide additional direct evidence for 1D facilitated diffusion prior to MutS mismatch identification.

ATP binding rapidly releases MutS from the mismatch

Including ATP or ATPγS with MutS and the +dT mismatch resulted in two distinct FRET states (Fig. 4a). The high FRET state displayed a FRET efficiency of 0.78 ± 0.15 (mean± s.d.) that appeared similar to MutS bound to the +dT mismatch in the absence of ATP (Fig. 4b). The second FRET state always occurred after the high FRET state and displayed an intermediate efficiency of 0.49 ± 0.17 (mean± s.d.) that appeared similar to the FRET efficiency obtained for facilitated diffusion along the duplex DNA (Fig. 4b). The dwell time of the high FRET state was inversely proportional to the concentration of ATP or ATPγS (Supplementary Fig. 7a, inset) and in saturating ATP ($\tau_{+dT\cdot on\cdot 1mMATP} = 3.0 \pm 0.2$ s, mean ± s.e.m.; Fig. 4c) is shorter by a factor of 12 than in the absence of ATP (Fig. 4d: Supplementary Fig. 7). A fractional Hill coefficient[23] is consistent with well–known asymmetric ATP binding activity of MutS ($n = 0.24 \pm 0.09$, mean ± s.e.m.; Supplementary Fig. 7a)[24]. The ATP/ATPγS–dependent change of the high mismatch–bound FRET state to the intermediate 1D diffusion FRET state strongly suggests the formation of a sliding clamp (Fig. 4a)[4],[25]. With a longer DNA substrate (100 bp) and a shorter time resolution (4 ms) we only observe the previously identified FRET states corresponding to mismatch searching, mismatch binding, and the formation of an ATP–bound MutS sliding clamp (Supplementary Fig. 6). These results suggest that additional significant MutS mismatch binding and clamp formation intermediates are unlikely.

ATP–bound MutS sliding clamps are extremely stable on DNA

The lifetime of ATP–bound MutS was examined by time–lapse FRET (Fig. 4d; Online Methods). Scans from a population of molecules were fit to a single exponential and the dwell times were calculated for sliding clamps in the presence of ATP ($\tau_{SC\cdot ATP} = 598 \pm 18$ s, mean ± s.e.m.) and ATPγS ($\tau_{SC\cdot ATP\gamma S} = 579 \pm 28$ s, mean ± s.e.m.; Fig. 4e). The near equivalent dwell times of MutS sliding clamps in the presence of ATP and ATPγS is not surprising since the rate of spontaneous ATPγS hyrolysis by MSH (~0.1 min^{-1})[26] appears equivalent to the MutS sliding clamp lifetime. Moreover, the dwell time varies by less than a factor of two over three orders–of–magnitude in ATP concentration (1–1000 μM), suggesting that the formation and stability of MutS sliding clamps does not involve ATP turnover (Supplementary Fig. 7b). In the absence of the external end–block the second intermediate FRET state decayed extremely fast (75% of the molecules $\tau_{SC\cdot ATP} < 30$ ms; 25% fit a single exponential with $\tau_{SC\cdot ATP} = 2.2 \pm 0.4$ s, mean ± s.e.m.; Supplementary Fig. 7c), suggesting that fully end blocked DNA is required to retain the MutS sliding

clamps[4],[25]. These results support the conclusion that ATP/ATPγS binding by MutS provokes the formation of an extremely stable hydrolysis–independent sliding clamp on DNA[4],[25]; lasting for ~10 min or 16–fold longer than on a mismatch and 160–fold longer than on duplex DNA. Moreover, the dwell time of ATP–bound MutS sliding clamps is insensitive to ionic strength (Supplementary Fig. 5c), suggesting that the 1D diffusion by ATP–bound MutS clamps is fundamentally distinct from lesion–scanning MutS clamps. We consider semi frictionless 1D diffusion similar to β–clamp/PCNA as a likely mechanism[27]. The use of ATP as an allosteric effector to radically bias the boundary conditions of Brownian diffusion appears to be an unambiguous case of RTB as a mechanism for signaling MMR[11],[12],[28].

Direct observation of multiple MutS sliding clamps

In spite of the relatively short DNA length and rapid facilitated diffusion of a single sliding clamp, we observed multiple sliding clamps on the same single molecule (Fig. 4f)[4],[25],[29]. The occurrence of multiple MutS proteins on a single DNA was easily distinguishable from a single MutS protein containing two Cy3 fluorophores (Supplementary Fig. 8). The frequency of more than one MutS on a single DNA molecule increased with protein concentration as well as DNA length and at physiological concentrations of MutS (300 nM) can account for nearly 75% of the single DNA molecules examined (Fig. 4f). Single DNA molecules with multiple MutS proteins appear to be formed rapidly and in many cases in linear succession with similar kinetics and lifetime to the binding and clamp formation of a single MutS (Supplementary Fig. 8). These results are consistent with the Molecular Switch model where multiple sliding clamps are used to clear the DNA surrounding a mismatch and recruit downstream MMR machinery such as MutL homologs (MLH/PMS)[4],[25],[29]–[31].

Single–Stranded DNA Induces the Release of MutS Sliding Clamps

The lifetime of ATP–bound MutS sliding clamps engenders an important question: how are they released? To address this issue, we examined MutS interaction with a +dT mismatched DNA containing a biotin–streptavidin blocked oligo dT_{10} single–stranded DNA (ssDNA) tail (Fig. 5a). In the presence of 200 μM ATP we observe a high efficiency FRET state (0.79 ± 0.12, mean ± s.d.; $\tau_{+dT-(dT10)\cdot on}$ = 4.8 ± 0.3 s, mean ± s.e.m.; Fig. 5b; compared to $\tau_{+dT\cdot on}$ = 5.0 ± 0.5 s, mean ± s.e.m. at 200 μM ATP; see Supplementary Fig. 6a, inset) that resolves to an intermediate FRET state (0.51± 0.17, mean ± s.d.; Fig. 5c) which is extremely short–lived compared to the +dT without an ssDNA tail ($\tau_{SC-(dT10)\cdot ATP}$ = 7.0 ± 0.7 s, mean ± s.e.m.; Fig. 5c; also see large < 30 ms population bin; compare to Fig. 4e). Substitution of ATPγS for ATP resulted in fewer protein–DNA interactions and a smaller < 30 ms bin but a qualitatively similar intermediate FRET dwell time ($\tau_{SC-(dT10)\cdot ATP\gamma S}$ = 8.6 ± 0.5 s, mean ± s.e.m.; Fig. 5d). We also observe an accelerated release of MutS from duplex DNA containing an oligo dT_{10} ssDNA tail that appeared similar to unblocked duplex DNA (Supplementary Fig. 9). These results are consistent with the conclusion that ssDNA enhances the release of MutS clamps. We consider the possibilities that ssDNA provokes ATP hydrolysis and clamp release and/or the ssDNA is less structured or does not provide the girth required to maintain MutS clamps.

DISCUSSION

The mechanism of MMR has been a controversial topic for well over a decade and is important since Lynch syndrome (hereditary non–polyposis colorectal cancer or LS/HNPCC) and a large number of sporadic colorectal, endometrial, ovarian and upper urinary tract tumors are accelerated by MMR defects[32],[33]. Much of the controversy can be traced to non–physiological biochemical conditions and crystal structures that appear to suggest only one form of MSH's[10],[11],[32–34]. Our real–time smFRET studies have identified two dynamically distinct clamp forms of MutS and place substantial kinetic restrictions that appear to be uniquely resolved by the Molecular Switch Model for MMR[4],[25],[29–31].

An important consideration for any model is how MutS proteins find a mismatch? Changes in FRET efficiency and distribution with length and time resolution indicated that MutS performs a mismatch search by rotational diffusion while in continuous contact with the duplex DNA (Fig. 2; Supplementary Fig. 4). Combined with an increased dissociation constant with a blocked–end duplex DNA and a 1 s dwell time at physiological ionic strength, our results suggest a search process that utilizes transient MutS scanning clamps to examine short DNA segments (~700 bp) and theoretical inter–strand 3D jumps to overcome chromatin blocks. This combination in concert with macromolecular crowding and DNA looping appears to provide the capacity to search an entire genome for DNA mismatches or lesions[34].

One of the most contentious issues is transmitting the recognition signal from the mismatch to the strand scission[3]. We find that mismatch–provoked ATP–binding results in distinctly different MutS sliding clamps that are stable on the DNA for nearly 10 min; a length of time equivalent to a complete MMR reaction[35],[36]. These extremely stable MutS clamps appear to represent the lasting signal for MMR[4],[25],[29–31], and provide unambiguous support for RTP in biology. A random walk 1D facilitated diffusion on naked DNA could transmit this mismatch identification signal ~20 kb. Considering reflecting barriers caused by iterative multiple sliding clamps (Fig. 4f), such a naked DNA signal could encompass up to 10^6 bp. However, cellular DNA is not naked and MSH sliding clamps appear capable of disassembling nucleosomes, which may assist in clearing the DNA surround a mismatch prior to excision[26]. Such supplementary activities and restrictions will undoubtedly reduce the effective distance of the MutS signal, perhaps to the 1–2 kb range observed for MMR.

A cis–MMR model has been considered that uses the energy of ATP–hydrolysis to motor from the mismatch to the strand scission[3]. It was argued that short experimental DNAs precluded the ability to observe direction–driven hydrolysis[37]. The extremely long lifetime and rapid appearance of multiple ATP–bound MutS sliding clamps places clear limits on this concept. One conceptual limit would seem to involve the kinetic organization of multiple sliding clamps into a complex capable of directional hydrolysis–driven translocation. A second limit would seem to be the ~10 min stability of MutS clamps on the DNA that is independent of ATP hydrolysis. Thus, either another protein such as MLH/PMS regulates the DNA contact and ATP hydrolysis, or a strand scission is encountered within this time. This latter possibility would appear identical to the Molecular Switch Model[4],[25],[29–31].

The release of MutS clamps by short ssDNA may resolve the final steps of the MMR mechanism (Fig. 6). Recognition of the mismatch requires short (1 s) duplex scans that may ultimately cover the entire genome in 1–10 min (Fig. 6a)[34]. One could envision a local increase in MMR components and associated scanning at a replication fork driven by β–clamp/PCNA interactions[38],[39]. In the presence of ATP, the residence time of MutS on the mismatch is 3 s (Fig. 6b); sufficient time to detect mismatch–associated DNA flexibility[40], interrogate the mismatch[41]–[43], and exchange adenosine nucleotide[29]. ATP binding results in the formation of an extremely stable MSH signaling clamp (~10 min) that may easily recruit MLH/PMS[4],[44] as well as the remaining excision repair machinery (Fig. 6b)[2]. A resulting short ssDNA excision tract associated with MMR would provoke release of the MSH–MLH/PMS clamp complex from the DNA (Fig. 6c)[45]. The excision repair reaction would be iteratively sustained with multiple sliding clamps until the mismatch is removed and the ssDNA tract releases any remaining clamps[4],[25],[29]–[31].

Complete methods may be found on–line.

Supplementary Material

Refer to Web version on PubMed Central for supplementary material.

Acknowledgments

References

1. Kolodner RD, Marsischky GT. Eukaryotic DNA mismatch repair. Current Opin Genet Dev. 1999; 9:89–96.

2. Modrich P, Lahue R. Mismatch repair in replication fidelity, genetic recombination, and cancer biology. Annu Rev Biochem. 1996; 65:101–33. [PubMed: 8811176]

3. Kolodner RD, Mendillo ML, Putnam CD. Coupling distant sites in DNA during DNA mismatch repair. Proc Natl Acad Sci U S A. 2007; 104:12953–4. [PubMed: 17664420]

4. Acharya S, Foster PL, Brooks P, Fishel R. The coordinated functions of the E. coli MutS and MutL proteins in mismatch repair. Mol Cell. 2003; 12:233–46. [PubMed: 12887908]

5. Gradia S, Acharya S, Fishel R. The role of mismatched nucleotides in activating the hMSH2–hMSH6 molecular switch. J Biol Chem. 2000; 275:3922–3930. [PubMed: 10660545]

6. Berg OG, Winter RB, von Hippel PH. Diffusion–driven mechanisms of protein translocation on nucleic acids. 1 Models and theory. Biochemistry. 1981; 20:6929–48. [PubMed: 7317363]

7. Riggs AD, Bourgeois S, Cohn M. The lac repressor–operator interaction. 3 Kinetic studies. J Mol Biol. 1970; 53:401–17. [PubMed: 4924006]

8. Blainey PC, van Oijen AM, Banerjee A, Verdine GL, Xie XS. A base–excision DNA–repair protein finds intrahelical lesion bases by fast sliding in contact with DNA. Proc Natl Acad Sci U S A. 2006; 103:5752–7. [PubMed: 16585517]

9. Gorman J, et al. Dynamic basis for one–dimensional DNA scanning by the mismatch repair complex Msh2–Msh6. Mol Cell. 2007; 28:359–70. [PubMed: 17996701]

10. Wolffe AP, Guschin D. Review: chromatin structural features and targets that regulate transcription. J Struct Biol. 2000; 129:102–22. [PubMed: 10806063]

11. Fox RF. Rectified Brownian movement in molecular and cell biology. Phys Rev E. 1998; 57:2177–2203.

12. Fox RF, Choi MH. Rectified Brownian motion and kinesin motion along microtubules. Phys Rev E Stat Nonlin Soft Matter Phys. 2001; 63:051901. [PubMed: 11414927]

13. Roy R, Hohng S, Ha T. A practical guide to single–molecule FRET. Nature Methods. 2008; 5:507–16. [PubMed: 18511918]

14. Biswas I, Hsieh P. Identification and characterization of a thermostable MutS homolog from Thermus aquaticus. J Biol Chem. 1996; 271:5040–8. [PubMed: 8617781]

15. Blanchard SC, Kim HD, Gonzalez RL Jr, Puglisi JD, Chu S. tRNA dynamics on the ribosome during translation. Proc Natl Acad Sci U S A. 2004; 101:12893–8. [PubMed: 15317937]

16. Murphy MC, Rasnik I, Cheng W, Lohman TM, Ha T. Probing single–stranded DNA conformational flexibility using fluorescence spectroscopy. Biophys J. 2004; 86:2530–7. [PubMed: 15041689]

17. Karran P, Hampson R. Genomic instability and tolerance to alkylating agents. Cancer Surveys. 1996; 28:69–85. [PubMed: 8977029]

18. Karran P, Marinus MG. Mismatch correction at O6–methylguanine residues in E. coli DNA Nature. 1982; 296:868–9.

19. Blainey PC, et al. Nonspecifically bound proteins spin while diffusing along DNA. Nat Struct Mol Biol. 2009; 16:1224–9. [PubMed: 19898474]

20. Tessmer I, et al. Mechanism of MutS searching for DNA mismatches and signaling repair. J Biol Chem. 2008; 283:36646–54. [PubMed: 18854319]

21. Schofield MJ, Nayak S, Scott TH, Du C, Hsieh P. Interaction of Escherichia coli MutS and MutL at a DNA mismatch. J Biol Chem. 2001; 276:28291–9. [PubMed: 11371566]

22. Yang Y, Sass LE, Du C, Hsieh P, Erie DA. Determination of protein–DNA binding constants and specificities from statistical analyses of single molecules: MutS–DNA interactions. Nucleic Acids Res. 2005; 33:4322–34. [PubMed: 16061937]

23. Abeliovich H. An empirical extremum principle for the hill coefficient in ligand–protein interactions showing negative cooperativity. Biophys J. 2005; 89:76–9. [PubMed: 15834004]

24. Lamers MH, Winterwerp HH, Sixma TK. The alternating ATPase domains of MutS control DNA mismatch repair. EMBO J. 2003; 22:746–56. [PubMed: 12554674]

25. Gradia S, et al. hMSH2–hMSH6 forms a hydrolysis–independent sliding clamp on mismatched DNA. Mol Cell. 1999; 3:255–61. [PubMed: 10078208]

26. Javaid S, et al. Nucleosome remodeling by hMSH2–hMSH6. Mol Cell. 2009; 36:1086–94. [PubMed: 20064472]

27. Laurence TA, et al. Motion of a DNA sliding clamp observed by single molecule fluorescence spectroscopy. J Biol Chem. 2008; 283:22895–906. [PubMed: 18556658]

28. Mather WH, Fox RF. Kinesin's biased stepping mechanism: amplification of neck linker zippering. Biophys J. 2006; 91:2416–26. [PubMed: 16844749]

29. Gradia S, Acharya S, Fishel R. The human mismatch recognition complex hMSH2–hMSH6 functions as a novel molecular switch. Cell. 1997; 91:995–1005. [PubMed: 9428522]

30. Fishel R. Mismatch repair, molecular switches, and signal transduction. Genes Dev. 1998; 12:2096–101. [PubMed: 9679053]

31. Fishel R. Signaling mismatch repair in cancer. Nature Med. 1999; 5:1239–1241. [PubMed: 10545986]

32. Fishel R. The selection for mismatch repair defects in hereditary nonpolyposis colorectal cancer: revising the mutator hypothesis. Cancer Res. 2001; 61:7369–74. [PubMed: 11606363]

33. Hampel H, et al. Screening for the Lynch syndrome (hereditary nonpolyposis colorectal cancer). N Engl J Med. 2005; 352:1851–60. [PubMed: 15872200]

34. Li G–W, Berg OG, Elf J. Effects of macromolecular crowding and DNA looping on gene regulation kinetics. Nature Phys. 2009; 5:294–297.

35. Constantin N, Dzantiev L, Kadyrov FA, Modrich P. Human mismatch repair: reconstitution of a nick directed bidirectional reaction. J Biol Chem. 2005; 280:39752–61. [PubMed: 16188885]

36. Lahue RS, Au KG, Modrich P. DNA mismatch correction in a defined system. Science. 1989; 245:160–4. [PubMed: 2665076]

37. Blackwell LJ, Martik D, Bjornson KP, Bjornson ES, Modrich P. Nucleotide–promoted release of hMutS alpha from heteroduplex DNA is consistent with an ATP–dependent translocation Mechanism. J Biol Chem. 1998; 273:32055–32062. [PubMed: 9822680]

38. Lau PJ, Kolodner RD. Transfer of the MSH2. MSH6 complex from proliferating cell nuclear antigen to mispaired bases in DNA. J Biol Chem. 2003; 278:14–7. [PubMed: 12435741]

39. Shell SS, Putnam CD, Kolodner RD. The N terminus of Saccharomyces cerevisiae Msh6 is an unstructured tether to PCNA. Mol Cell. 2007; 26:565–78. [PubMed: 17531814]

40. Mazurek A, Johnson CN, Germann MW, Fishel R. Sequence context effect for hMSH2–hMSH6 mismatc–dependent activation. Proc Natl Acad Sci U S A. 2009; 106:4177–82. [PubMed: 19237577]

41. Lamers MH, et al. The crystal structure of DNA mismatch repair protein MutS binding to a G x T mismatch. Nature. 2000; 407:711–7. [PubMed: 11048711]

42. Obmolova G, Ban C, Hsieh P, Yang W. Crystal structures of mismatch repair protein MutS and its complex with a substrate DNA. Nature. 2000; 407:703–10. [PubMed: 11048710]

43. Warren JJ, et al. Structure of the human MutSalpha DNA lesion recognition complex. Mol Cell. 2007; 26:579–92. [PubMed: 17531815]

44. Mendillo ML, Mazur DJ, Kolodner RD. Analysis of the interaction between the Saccharomyces cerevisiae MSH2–MSH6 and MLH1–PMS1 complexes with DNA using a reversible DNA end–blocking system. J Biol Chem. 2005; 280:22245–57. [PubMed: 15811858]

45. Heo SD, Cho M, Ku JK, Ban C. Steady–state ATPase activity of E. coli MutS modulated by its dissociation from heteroduplex DNA. Biochem Biophys Res Commun. 2007; 364:264–9. [PubMed: 17950245]

46. Cho M, Chung S, Heo SD, Ku J, Ban C. A simple fluorescent method for detecting mismatched DNAs using a MutS–fluorophore conjugate. Biosens Bioelectron. 2007; 22:1376–81. [PubMed: 16876990]

47. Rasnik I, Myong S, Cheng W, Lohman TM, Ha T. DNA–binding orientation and domain conformation of the E. coli rep helicase monomer bound to a partial duplex junction: single–molecule studies of fluorescently labeled enzymes. J Mol Biol. 2004; 336:395–408. [PubMed: 14757053]

48. Joo, C.; Ha, T. Single–molecule FRET with total internal reflection microscopy. In: Selvin, PR.; Ha, T., editors. Single–molecule techniques: A laboratory manual. Cold Spring Harbor Laboratory Press; Cold Spring Harbor: 2008.
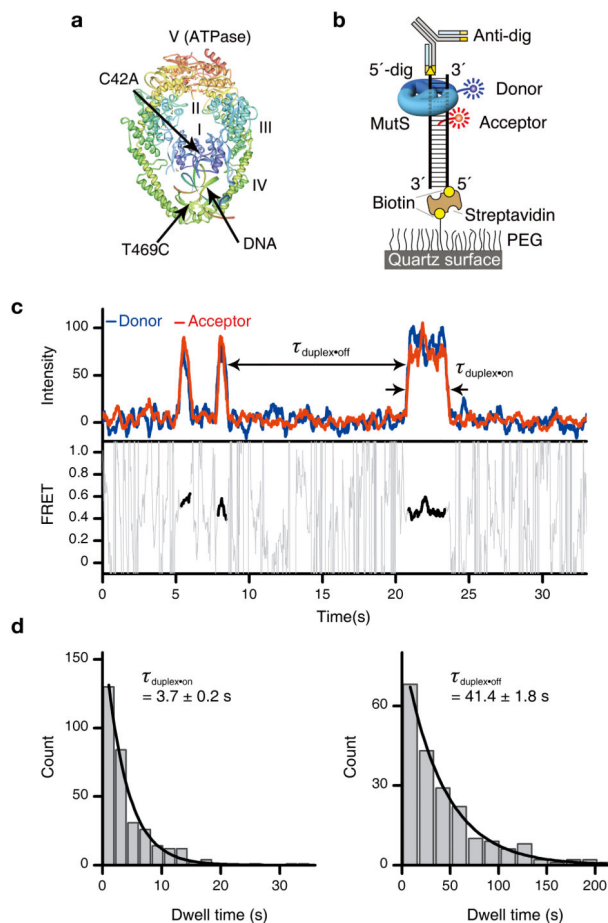
Figure 1. Single–molecule FRET of *Taq* MutS on duplex DNA
(a) The crystal structure of homodimer *Taq* MutS bound to unpaired dT (PDB:1EWQ)[42]. Donor Cy3 was conjugated to C469 of *Taq* MutS(C42A, T469C). **(b)** Schematic representation of smFRET assay. Cy5–labeled matched DNA molecules (74 bp) were immobilized on a quartz surface via a biotin–streptavidin linker and the open–end blocked antidigoxigenin. (**c**) Representative traces of fluorescent intensity and FRET efficiency for matched DNA molecules in the presence of 10 nM MutS and 100 mM KCl. (**d**) The distributions of binding lifetime and dissociation time for 10 nM MutS in 100 mM KCl. A single exponential with mean ± s.e.m. fit the distribution.
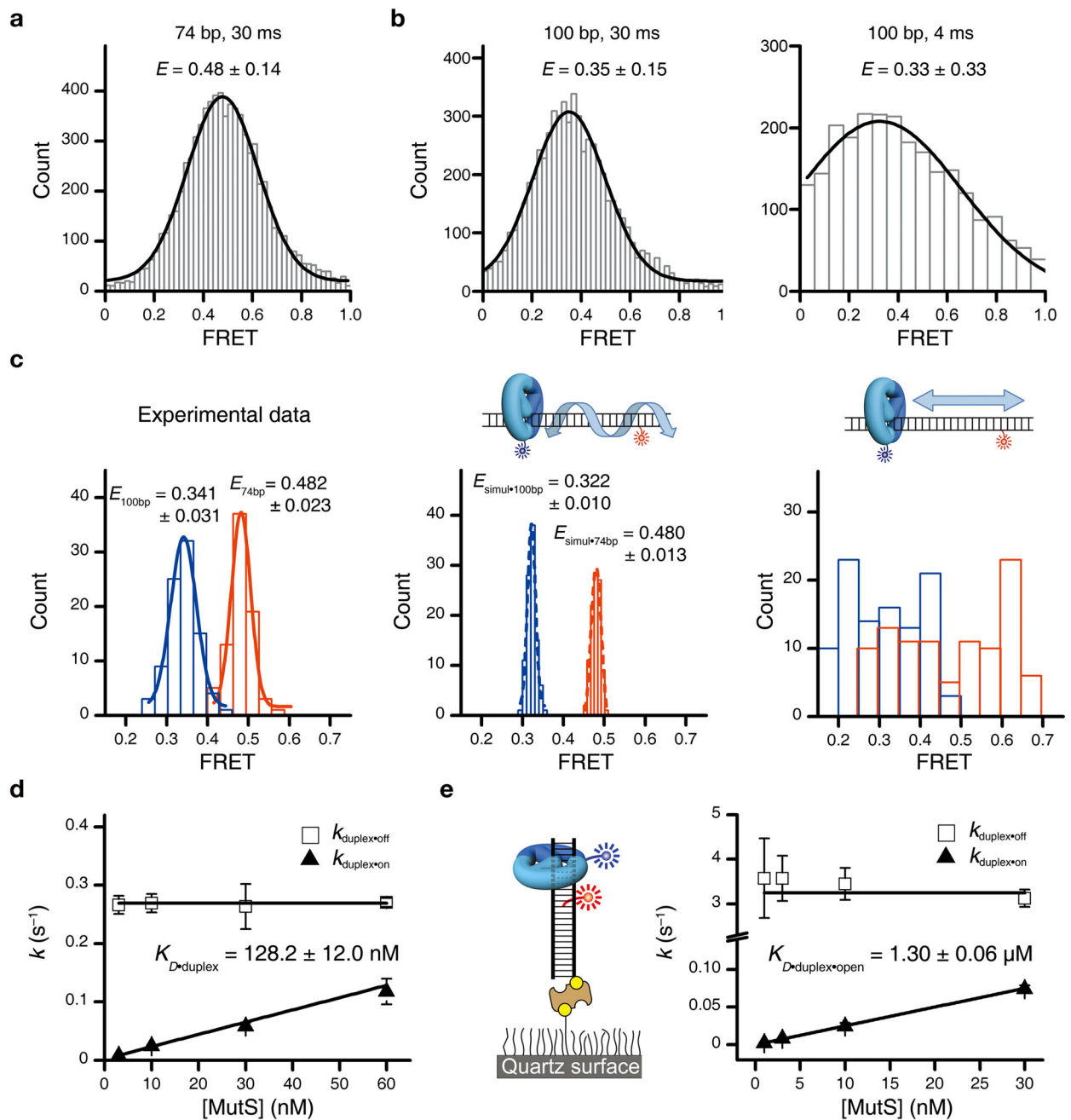
Figure 2. *Taq* **MutS scans duplex DNA by rotational diffusion**

(**a**) FRET efficiency determined from a population histogram of 74 bp duplex DNA molecules at a 30 ms time resolution. (**b**) FRET efficiency determined from a population histogram of 100 bp duplex DNA molecules at a 30 ms time resolution and 4 ms time resolution, respectively. (**c**) Averaged FRET value from individual traces of MutS diffusion on duplex DNA was determined. The Gaussian distribution of the FRET efficiency resulted in a refined FRET efficiency of 0.481 ± 0.023 (mean $\pm$ s.d.) on the 74 bp duplex DNA (n = 78) and 0.341 ± 0.031 (mean $\pm$ s.d.) on the 100 bp duplex DNA (n = 89) (left panel). For the transitional diffusion model, the circumference distance between Cy3 and Cy5 determined

by the random initial binding remains constant during MutS diffusion. The distributions of FRET efficiency were obtained from 100 trials *in silico* of the arbitrary binding position of MutS for the 74 bp and 100 bp duplex DNAs, which evenly range from 0.291 to 0.655 and 0.199 to 0.443, respectively (right panel). In contrast, the circumference distance varies with rotational diffusion in the rotational diffusion model (middle panel). The resulting distribution of FRET values displays a Gaussian with a sharp peak (0.479 ± 0.007 for 74 bp; 0.322 ± 0.011 for 100 bp). The errors indicate s.d. **(d)** The dissociation constant with blocked ends was determined from the intercept of $\tau_{\text{duplex·on}}$ and $\tau_{\text{duplex·off}}$ for MutS binding to duplex DNA. **(e)** The dissociation constant with an open–ended DNA was determined from the intercept of $\tau_{\text{duplex·on}}$ and $\tau_{\text{duplex·off}}$ for MutS binding to $3'$ –unblocked duplex DNA.
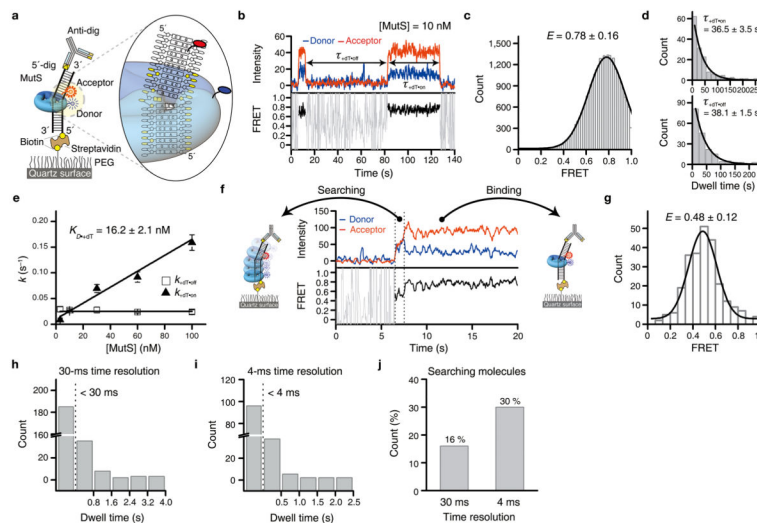
Figure 3. Single–molecule FRET of *Taq* MutS binding to a +dT mismatch

(**a**) Schematic illustration of mismatched DNA molecules containing a single unpaired +dT. Cy5 is positioned at the ninth base from the +dT mismatch. Yellow indicates nucleotides that contact MutS residues during mismatch binding[41]–[43]. (**b**) Representative traces of fluorescence intensity and FRET value for a +dT mismatch in the presence of 10 nM MutS and 100 mM KCl. (**c**) FRET efficiency when MutS was bound to the +dT mismatch. (**d**) The distributions of MutS binding lifetime and dissociation time for 10 nM MutS in 100 mM KCl. A single exponential with mean ± s.e.m. fit the distribution. (**e**) On–rate ($k_{+dT \cdot on} = 1/\tau_{+dT \cdot off}$) and off–rate ($k_{+dT \cdot off} = 1/\tau_{+dT \cdot on}$) vs. concentration of *Taq* MutS. The dissociation constant was determined at the intercept of $\tau_{duplex \cdot on}$ and $\tau_{duplex \cdot off}$ for MutS binding to a +dT mismatch. (**f**) Representative trace of fluorescent intensity and FRET value showing the searching kinetics followed by binding kinetics for a +dT mismatch. (**g**) FRET efficiency when MutS is searching for a mismatch. (**h**) The distributions of binding lifetime for MutS in search of a mismatch at a 30 ms time resolution. (**i**) The distributions of binding lifetime for MutS in search of a mismatch at a 4 ms time resolution. (**j**) The frequency of single molecules where MutS is found searching for a mismatch at a 30 ms and 4 ms time resolution.
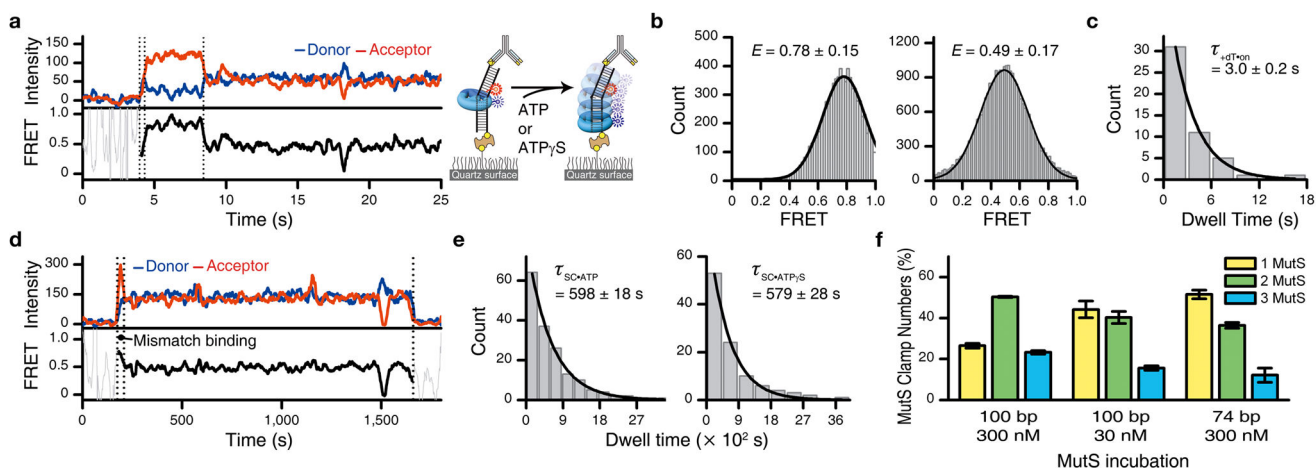
Figure 4. ATP induces an exceptionally long–lived FRET state of MutS
(**a**) Schematic representation of ATP/ATPγS effects on mismatch bound MutS and Representative traces of fluorescence intensity and FRET value for a +dT mismatch in the presence of 10 nM MutS, 100 mM KCl and 200 μM ATP. (**b**) High FRET efficiency and intermediate FRET efficiency determined from a population histogram of +dT mismatched DNA molecules. (**c**) The distributions of MutS binding lifetime to a +dT mismatch in the presence of 1 mM ATP. (**d**) Representative time–lapse trace of ATP–bound *Taq* MutS on the +dT mismatched DNA substrate. (**e**) Dwell time of the intermediate FRET state of MutS in the presence of ATP and ATPγS determined from a single exponential of a population histogram of +dT molecules. (**f**) The frequency of one (yellow), two (green), and three (blue) MutS sliding clamps found on 100 bp and 74 bp single DNA molecules in the presence of 30 nM or 300 nM MutS.
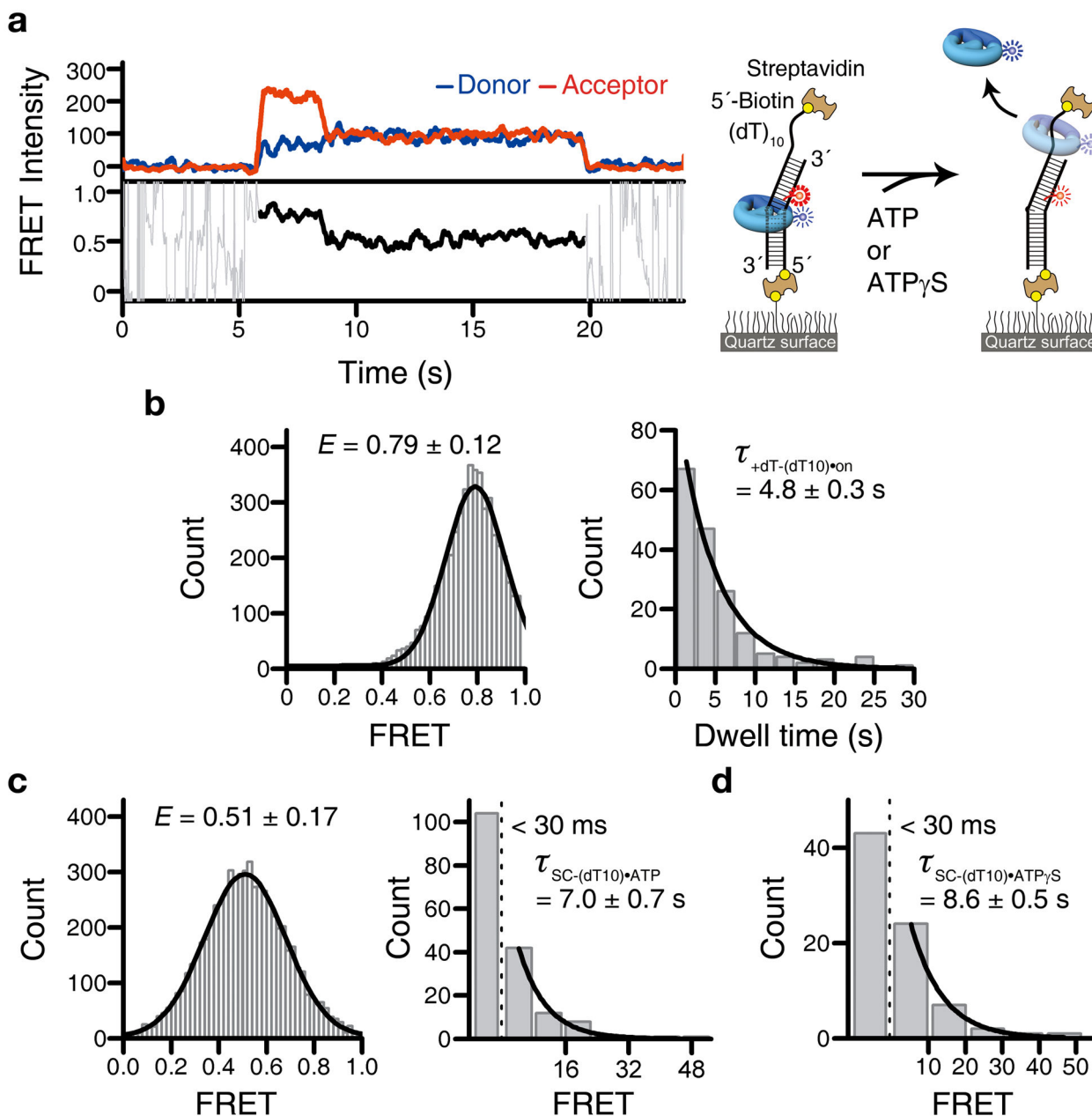
Figure 5. Single–stranded DNA provokes the release of ATP–bound MutS Sliding Clamps
(a) Representative traces of fluorescence intensity and FRET value for a +dT mismatch containing a $(dT)_{10}$ single–stranded DNA 5′–tail in the presence of 10 nM MutS, 100 mM KCl, and 200 μM ATP. Schematic representation of +dT mismatch containing a $(dT)_{10}$ single–stranded DNA 5′–tail with MutS and ATP/ATPγS. **(b)** The distributions of FRET efficiency and binding lifetime determined from a population histogram of +dT–$(dT)_{10}$ DNA molecules. **(c)** The distributions of FRET efficiency and binding lifetime determined from a population histogram of +dT–$(dT)_{10}$ DNA molecules in the presence of 200 μM ATP. **(d)** The distributions of binding lifetime determined from a histogram of +dT–$(dT)_{10}$ DNA molecules in the presence of 200 μM ATPγS.
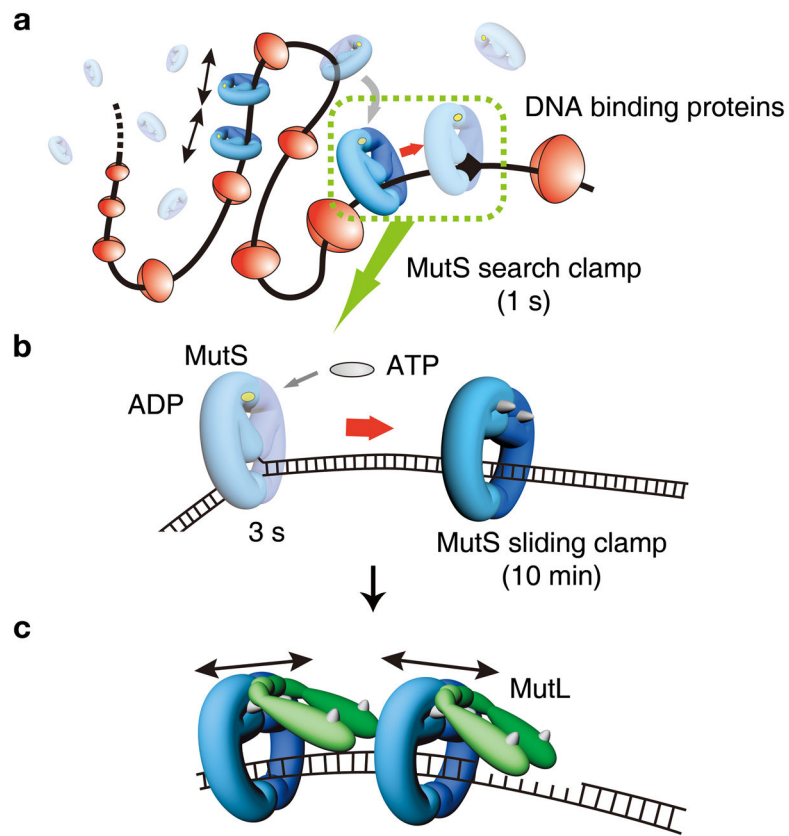
Figure 6. The role of distinct MutS clamps in the Molecular Switch Model for MMR
(a) MutS searching clamps. **(b)** MutS mismatch binding and sliding clamps. **(c)** MutS–MutL complexes with an MMR excision tract that provokes the release of MutS sliding clamps.